Measurement of fusion evaporation residue cross sections in the ^{48}Ti + ^{138}Ba reaction

K. K. Rajesh,[1,*] M. M. Musthafa,[1] N. Madhavan,[2] S. Nath,[2] J. Gehlot,[2] Jhilam Sadhukhan,[3] P. Mohamed Aslam,[1] P. T. Muhammed shan,[1] E. Prasad,[4] M. M. Hosamani,[5] T. Varughese,[2] Abhishek Yadav,[6] Vijay R. Sharma,[2,†] Vishal Srivastava,[2,7] Md. Moin Shaikh,[3] M. Shareef,[4] A. Shamlath,[4] and P. V. Laveen[4]

[1]*Department of Physics, University of Calicut, Malappuram - 673635, India*
[2]*Inter University Accelerator Centre, Aruna Asaf Ali Marg, New Delhi 110067, India*
[3]*Variable Energy Cyclotron Centre, 1/AF Bidhan Nagar, Kolkata 700 064, India*
[4]*Department of Physics, School of Physical Sciences, Central University of Kerala,Kasaragod 671314, India*
[5]*Department of Physics, Karnatak University, Dharwad 580003, India*
[6]*Department of Physics, Jamia Millia Islamia, New Delhi 110025, India*
[7]*The Racah Institute of Physics, The Hebrew University of Jerusalem, Jerusalem 91904, Israel*

(Received 27 December 2018; revised manuscript received 5 August 2019; published 22 October 2019)

Evaporation residue cross sections are measured for the reaction ^{48}Ti + ^{138}Ba which forms the compound nucleus ^{186}Pt*. The cross sections are measured at beam energies in the range of 189.3–234.4 MeV. The experimental evaporation residue cross sections are compared with the dynamical model which employs one-dimensional Langevin dynamical calculations. The dissipation strength of the Langevin equation is calculated using both chaos weighted wall formula and a constant reduced dissipation function. The measured ER cross sections are found to be much less than the theoretical predictions. Further, the measured ER cross sections for the system ^{48}Ti + ^{138}Ba are compared with those of ^{32}S + ^{154}Sm forming the same compound nucleus. The suppression in the evaporation residue cross sections of the former reaction may be attributed to the increasing competition from quasifission. The quasifission reaction is found to have superseded any effect of neutron shell closure ($N = 82$) of the target in the present study.

DOI: 10.1103/PhysRevC.100.044611

I. INTRODUCTION

The synthesis of heavier elements using heavy ion beams is severely hindered by fission and fission-like processes [1,2]. Experimental efforts for the formation of such elements are extremely challenging as evaporation residues (ER) for such reactions are heavily suppressed by a nonequilibrium process called quasifission (QF) [3–5]. In the case of QF, after the capture of projectile by the target nuclei, the system reseparates before the formation of a completely equilibrated compound nucleus (CN). The investigation into the major factors promoting this reseparation is not yet complete. Thus, a deep understanding of the various factors that can suppress a non-compound-nuclear reaction like QF and the techniques to enhance the production of super heavy elements (SHE) are the need of the hour.

The main evidence for QF are (i) strong mass-angle correlation in the mass-angle distribution of fission fragments [6–8], (ii) broader mass distributions compared to that of CN fission [7–10], (iii) anomalously large angular anisotropies compared to statistical model predictions [11–13], (iv) lower ER yield [9,14], and (v) unexpected γ ray multiplicity [15]. The presence of any of these signatures will indicate the reaction to be QF. The competition between fusion and QF determines the probability of formation of a completely equilibrated CN.

The major factors that influence QF process are entrance channel mass asymmetry [9,16–18], deformation of colliding partners [6,19–21], shell closure effect [22,23], and neutron excess of projectile and target [14]. Among the factors influencing QF, the entrance channel mass asymmetry is closely related to the product of projectile and target atomic numbers Z_pZ_t (where Z_p is the atomic number of projectile and Z_t is the atomic number of target) [7]. The dynamical models have predicted the onset of QF when the charge product $Z_pZ_t >$ 1600 [3]. However, the onset of QF has been reported for the systems even with charge product $Z_pZ_t \sim 540$ [24–26].

The pre-equilibrium model suggests that, in heavy ion induced reactions, in addition to normal fusion-fission process, a significant fraction of the non-compound-nuclear reaction is also present [27]. According to this model, if the critical mass asymmetry (α) is greater than the Businaro-Gallone mass asymmetry (α_{BG}) then the flux flow is from the lighter nucleus to heavier nucleus and it leads to CN formation. On the other hand, if $\alpha < \alpha_{BG}$, the flux flow is from heavier to lighter nucleus and the system reseparates before the formation of CN. However, contradicting results are also reported where $\alpha < \alpha_{BG}$ results in fusion-fission and $\alpha > \alpha_{BG}$ leads to QF [28].

In a classical experiment for the production of ^{293,294}Ts through ^{48}Ca induced reaction on ^{249}Bk, it required 70 d of beam time to detect one nucleus [29]. The cross section for the reaction is less than 1 pb. The main reason for the hindrance

*rajeshmlpm@yahoo.com
†Present address: Departamento del Acelerador, Instituto Nacional de Investigaciones Nucleares, Mexico.

TABLE I. Relevant parameters of projectile and target such as deformation, number of neutrons, and excitation energy of 2^+ excited state.

Nucleus	β_2	Neutrons	E_2^+ (MeV)
^{48}Ti	+0.276	26	0.984
^{138}Ba	+0.093	82	1.436

of the fusion cross section is attributed to QF. In the dinuclear system (DNS) model of nuclear fission, the probability of complete fusion ($P_{\rm CN}$) after the capture of projectile by target is highly dependent on the extent of QF. For the production of SHE, the current challenge is to understand the factors that influence $P_{\rm CN}$ [30].

The above discussion suggests that even though QF is a robust competitor to the fusion reaction involving heavy nuclei, a complete picture of the dynamics of QF is not yet known. To understand the extent of this non-compound-nuclear reaction in fusion dynamics, systematic measurements of ER cross sections are carried out for the reaction ^{48}Ti + ^{138}Ba forming ^{186}Pt* compound nucleus. Relevant parameters of the projectile and target are given in Table I. We are also interested to study if there is any enhanced survival probability of CN, due to the neutron shell closure ($N = 82$) of the target, is present. The paper is organized as follows. A detailed description of experimental set up is given in Sec. II. Data analysis can be found in Sec. III, and Sec. IV deals with experimental results. Theoretical calculations of the reaction is included in Sec. V. A general discussion of the implications of present study is under Sec. VI, while Sec. VII is devoted for summary.

II. EXPERIMENTAL DETAILS

The ER excitation function measurements are performed at Inter University Accelerator Centre (IUAC), New Delhi, using Pelletron+LINAC accelerator facility. Isotopically enriched (99.8%) thin targets of ^{138}Ba of thickness 200 μg/cm^2 were used in the experiment. In order to protect ^{138}Ba from oxidation, it is sandwiched between carbon films of backing thickness ≈20 μg/cm^2 and capping thickness ≈10 μg/cm^2 with carbon backing facing the beam. The fabrication of the target has already been reported [31]. The heavy ERs formed in the experiment are separated from the enormous beam background using hybrid recoil mass analyser (HYRA) operated in the gas-filled mode [32,33]. The electromagnetic configuration of first stage of HYRA is Q1Q2-MD1-Q3-MD2-Q4Q5, where Q is magnetic quadrupole and MD is magnetic dipole. This first stage is operated in momentum dispersive mode in the gas-filled mode of operation. The presence of MD1 and MD2 increase the rejection of primary and scattered beam as well as target-like particles at the focal plane [32]. This is achieved by the proper choice of the field values which ensures that only ERs reach the focal plane. The pressure of He gas is optimized at 0.3 Torr for the present experiment. The gas-filled region of HYRA is separated from the vacuum region using ≈660 μg/cm^2 window foil of carbon. In order to optimize the field values of the magnets, field scanning is done within a range of ±10% in steps of 2% of the calculated values of energy [34].

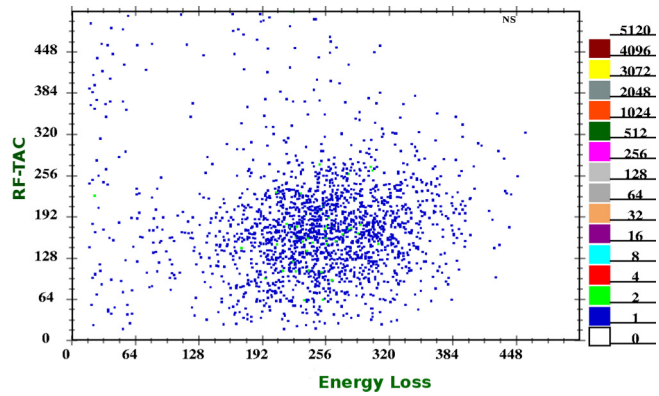

FIG. 1. A two-dimensional energy loss versus timing (or time of arrival of ERs) plot for the laboratory energy 241 MeV.

The measurements were performed at laboratory beam energies of 189.3, 195.5, 201.7, 208.9, 215.7, 224.0, and 234.4 MeV. The above energies were determined after correcting for the energy loss of the beam particles in 660 μg/cm^2 pressure window foil, 0.30 Torr of He gas between pressure window foil and target (≈35 cm), 20 μg/cm^2 carbon backing and 100 μg/cm^2 half thickness of ^{138}Ba. A position sensitive multiwire proportional counter (MWPC) of dimensions 6 in. × 2 in. detects the ERs reaching the focal plane [35]. In order to detect elastically scattered particles from the target, two silicon detectors were placed inside the target chamber at $\theta = \pm 25^\circ$. These detectors are also used to focus the beam at the center of the the target and to normalize ER cross sections.

The MWPC counts are used for the measurement of ER cross sections. A polypropelene foil of thickness 0.5 μm separates HYRA electromagnetic section from the focal plane. The detector is operated using isobutane gas at 2.5 mbar pressure and provides position (X_L, X_R, Y_U, and Y_D) signals, energy loss (ΔE) and timing signal. The position signals are processed through the constant fraction discriminator (CFD) and are fed to the time to digital converter (TDC) as stop signal, with anode signal as the common start. Energy signals (which are from the MWPC cathode and monitors) are fed to an analog to digital converter (ADC) for further processing. The logical OR signal of monitors and MWPC anode act as master strobe for the data acquisition system. A timing (on time of arrival) spectrum is generated using the timing pulse from the MWPC anode signal as the start signal and a suitably delayed radio frequency (RF) pulse as the stop signal. An energy loss versus timing plot with 250 ns pulse separation for a laboratory energy of 241 MeV is shown in Fig. 1. Data were collected and analyzed using IUAC data sorting software CANDLE [36].

III. DATA ANALYSIS

The total ER cross section can be calculated using the formula

$$\sigma_{\rm ER} = \left(\frac{Y_{\rm ER}}{Y_{\rm Mon}}\right)\left(\frac{d\sigma}{d\Omega}\right)\Omega_M \frac{1}{\eta_{\rm HYRA}}. \quad (1)$$

TABLE II. The different physical parameters such as potential barrier, critical mass asymmetry parameter, charge product, mean fissility, and fission barrier for the reactions ^{48}Ti + ^{138}Ba and ^{32}S + ^{154}Sm (which is the asymmetric reaction used for the comparison of ERs.), both forming same compound nucleus ^{186}Pt*.

Reaction	V_b(MeV)	α	Z_pZ_t	χ_m	B_f(MeV)
^{48}Ti + ^{138}Ba	141.3	0.483	1232	0.66	16.3
^{32}S + ^{154}Sm	115.3	0.656	992	0.54	16.3

Here, $Y_{\rm ER}$ is the ER yield at the focal plane, $Y_{\rm Mon}$ is the yield of elastically scattered particles recorded by the monitor detector, $d\sigma/d\Omega$ is the differential Rutherford scattering cross section in the laboratory frame, Ω_M is the solid angle subtended by the monitor detector, and $\eta_{\rm HYRA}$ is the transmission efficiency of the separator. The focal plane yield $Y_{\rm ER}$ is obtained from a two-dimensional energy loss versus time of arrival plot. The yield of the monitor detectors $Y_{\rm Mon}$ in the target chamber is obtained from the one dimensional spectrum using CANDLE software. The differential Rutherford scattering cross section can be calculated from the formula

$$\left(\frac{d\sigma}{d\Omega}\right) = 1.296\left(\frac{Z_pZ_t}{E_{\rm lab}}\right)^2\left[\frac{1}{\sin^4(\frac{\theta}{2})} - 2\left(\frac{A_p}{A_t}\right)^2 + \cdots\right], \quad (2)$$

where Z_p, Z_t and A_p, A_t are the atomic and mass numbers of the projectile and target, respectively. $E_{\rm lab}$ and θ are the energy of the incident projectile and scattering angle of the projectile-like particles in the laboratory frame of reference, respectively. The value of Z_pZ_t and other physical parameters are shown in Table II.

The extraction of transmission efficiency is very crucial in the measurement of cross sections. The transmission efficiency is the ratio of number of ERs reaching the focal plane of HYRA to the total number of ERs produced in the reaction. Transmission efficiency depends on several parameters such as the entrance channel mass asymmetry, beam energy, target thickness, the exit channel of interest, angular acceptance of the separator, magnetic field strengths, pressure of gas, etc. [33,37–39]. The transmission efficiency of ^{48}Ti induced reactions in the experimental facility of HYRA has already been reported [40]. We use the ^{48}Ti + ^{142}Nd reaction [40] as the calibration reaction to estimate the transmission efficiency of the present system.

To calculate the transmission efficiency, statistical model code PACE4 [41] is used to find the different possible ER channels and their relative yields in the reaction ^{48}Ti + ^{138}Ba, which are used for the normalization of the angular distribution. The ER angular distribution for this system is simulated using Monte Carlo simulation code TERS [34] at each energy point. This semimicroscopic code takes the actual input parameters during the experiment like neutron, proton, α separation energies, etc. The interaction of the beam with target is calculated event by event and it generates the reaction distribution of ERs such as angle, energy and charge state in the output. Here, due to focusing effects, energy and charge state are assumed nearly 100%, but practically the polar acceptance angle of HYRA is 9.5°. The average area under the curve up to 9.5° is considered in the calculations. The normalized angular distributions at each energy is obtained by adding the individual ER angular distributions with proper weighted yield. The normalized distributions obtained are shown in Fig. 2. It has been found that just below and above the Coulomb barrier, the ERs with *xn* decay channels diminish within an angle of 3.5 degrees from the beam axis while the ERs with α evaporation channels continue to increase up to 5 degrees. This results in the formation of two peaks in the normalized angular distribution. However, at higher excitation energies, ERs with *xn* evaporation channels are present even at larger angles. Hence it gives a continuum at higher excitation energies. A multiplication factor is obtained by taking the ratio of area under the curve using ^{48}Ti + ^{138}Ba and ^{48}Ti + ^{142}Nd calibration reaction up to 9.5°. The transmission efficiency value for ^{48}Ti + ^{138}Ba is extracted by multiplying $\eta_{\rm HYRA}$ for ^{48}Ti + ^{142}Nd with the multiplication factor. This way the transmission efficiency extracted for ^{48}Ti + ^{138}Ba is 28.7% ± 4.3%

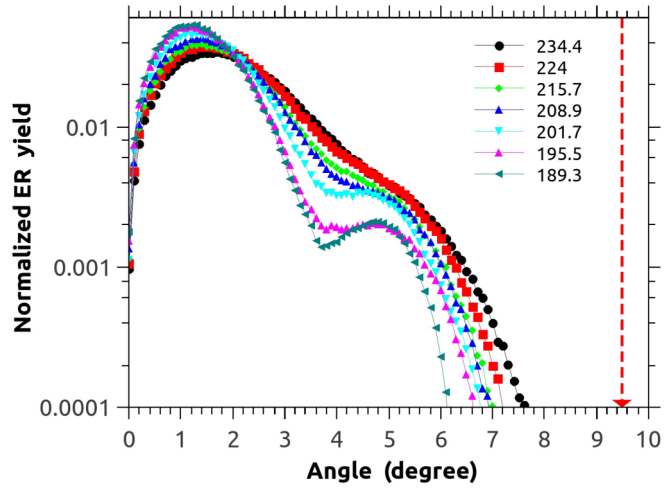

FIG. 2. Normalized angular distributions of ERs are simulated using TERS code. The angular acceptance of HYRA is 9.5° and is shown as a dashed arrow mark.

IV. EXPERIMENTAL RESULTS

The total ER cross section ($\sigma_{\rm ER}$) obtained as a function of center of mass energy ($E_{\rm c.m.}$) is shown in Fig. 3. The overall error in the calculated cross section is ∼15%. The measured excitation function shows a decreasing trend at higher beam energies. Generally, the competition from fission reduces the ER formation. A detailed study into the reasons that hinder the ER formation in the present reaction is performed in Sec. VI. The measured ER cross section for each center of mass energy along with corresponding excitation energy is shown in Table III. In the subsequent section, it can be seen that statistical model predictions do not reproduce experimental data.

V. THEORETICAL ANALYSIS

Dynamical model calculation is performed to reproduce the measured ER cross sections. In this calculation, we

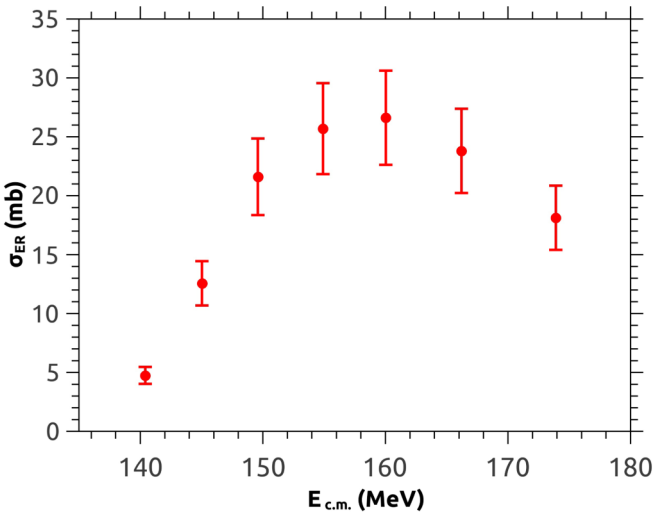

FIG. 3. Total ER cross sections as a function of center of mass energy. Beyond 160 MeV, there is a sharp fall in the ER cross sections.

have neglected the possibility of noncompound processes. Hence, any discrepancy with the experimental data can be attributed to the presence of noncompound reactions. We solve one-dimensional Langevin equations [42–44] which can be written as

$$\frac{dp}{dt} = -\frac{p^2}{2}\frac{\partial}{\partial c}\left(\frac{1}{m(c)}\right) - \frac{\partial F}{\partial c} - \frac{\eta(c)}{m(c)}p + g\Gamma(t),$$
$$\frac{dc}{dt} = \frac{p}{m(c)}, \tag{3}$$

where the "funny-hills" shape parameter c, representing the elongation of a nucleus, is used as the collective coordinate, and p is the momenta conjugate to c. The strength of the random force, g, is related to the friction coefficient η through fluctuation-dissipation theorem: $g = \sqrt{\eta T}$ [44]. The shape-dependent collective inertia $m(c)$ is extracted using Werner-Wheeler approximation [45,46] for the irrotational flow of incompressible nuclear fluid. The $\Gamma(t)$ represents the random force with the time correlation property $\langle\Gamma(t)\rangle = 0$ and $\langle\Gamma(t_1).\Gamma(t_2)\rangle = \delta(t_1 - t_2)$. The Helmholtz free energy $F = V - (a - a_0)T^2$ is used as the driving force for the collective motion; V and a being the deformation dependent potential energy and level density parameter [47], respectively. a_0 is

TABLE III. Measured ER cross sections as a function of center of mass energy and corresponding excitation energy

$E_{\text{c.m.}}$(MeV)	E^*(MeV)	σ_{ER}(mb)
140.4	41.51	4.8 ± 0.7
145.04	46.15	12.6 ± 1.9
149.6	50.71	21.6 ± 3.2
154.9	56.01	25.7 ± 3.9
160.03	61.14	26.6 ± 4.0
166.2	67.31	23.8 ± 3.6
173.9	75.01	18.1 ± 2.7

TABLE IV. CCFULL parameters used in the calculations of ^{48}Ti + ^{138}Ba and ^{32}S + ^{154}Sm reactions.

Reaction	V_0(MeV)	a_0(fm)	$r_0(fm)$
^{48}Ti+^{138}Ba	79.85	0.685	1.18
^{32}S+^{154}Sm	75.7	0.689	1.18

the value of a at the ground-state deformation. Temperature T is obtained from the ground-state excitation energy E^* as $T = \sqrt{E^*/a_0}$. V is calculated following the double-folding Yukawa-plus-exponential model [48].

Large number of Langevin events are simulated and finally an ensemble average has been taken to extract the experimental observables. The initial angular momentum for each event is sampled from the spin distribution of partial capture cross-section calculated using the CCFULL code [49]. The details of the CCFULL parameters are discussed in Table IV. Alternatively, we can use the fusion spin distribution given by

$$\frac{d\sigma(\ell)}{d\ell} = \frac{\pi}{k^2}\frac{(2\ell+1)}{1+\exp\left(\frac{\ell-\ell_c}{\delta\ell}\right)}, \tag{4}$$

where k is the wave number for the relative motion of the target-projectile combination. Here, ℓ_c and $\delta\ell$ are obtained from the systematics given in Ref. [43]. After obtaining the initial angular momentum, the potential energy is corrected with the corresponding rotational energy. The initial collective coordinate of the CN is considered to be the ground state deformation of the rotating nucleus. The initial momentum is obtained from the distribution of a thermally equilibrated system. A Langevin trajectory is considered to undergo fission when it crosses the scission point. We choose the scission configuration to correspond to a neck radius of $0.3R$, where R is the radius of the initial shape of the compound nucleus [50]. Possibilities of n, p, α, and γ evaporations are taken into account during the dynamical evolution. A Monte Carlo sampling is performed for this purpose at each time step of the Langevin propagation. The emission probabilities of these light particles [43,51] and γ rays [43,52] are calculated using the standard statistical model formula. In case evaporation occurs, the CN and other dynamical quantities, like angular momentum and excitation energy of the composite, are updated to the corresponding daughter nucleus. An event is assigned to be an evaporation residue when the excitation energy reduces below the fission barrier. Therefore, if N_f is the number of fission events out of N_t Langevin trajectories of an ensemble, then the ER cross section is defined as

$$\sigma_{\text{ER}} = \sigma_{fu}\left(\frac{N_t - N_f}{N_t}\right), \tag{5}$$

where σ_{fu} is the fusion cross section extracted by integrating Eq. (4).

We have used the shape-dependent chaos-weighted wall friction (CWWF) [53] for the dissipation strength η. ER cross section is calculated for the present reaction and is plotted in Fig. 4(a) as a function of excitation energy. The calculated results strongly overestimate the experimental data for the system. In order to see the effect on a less symmetric

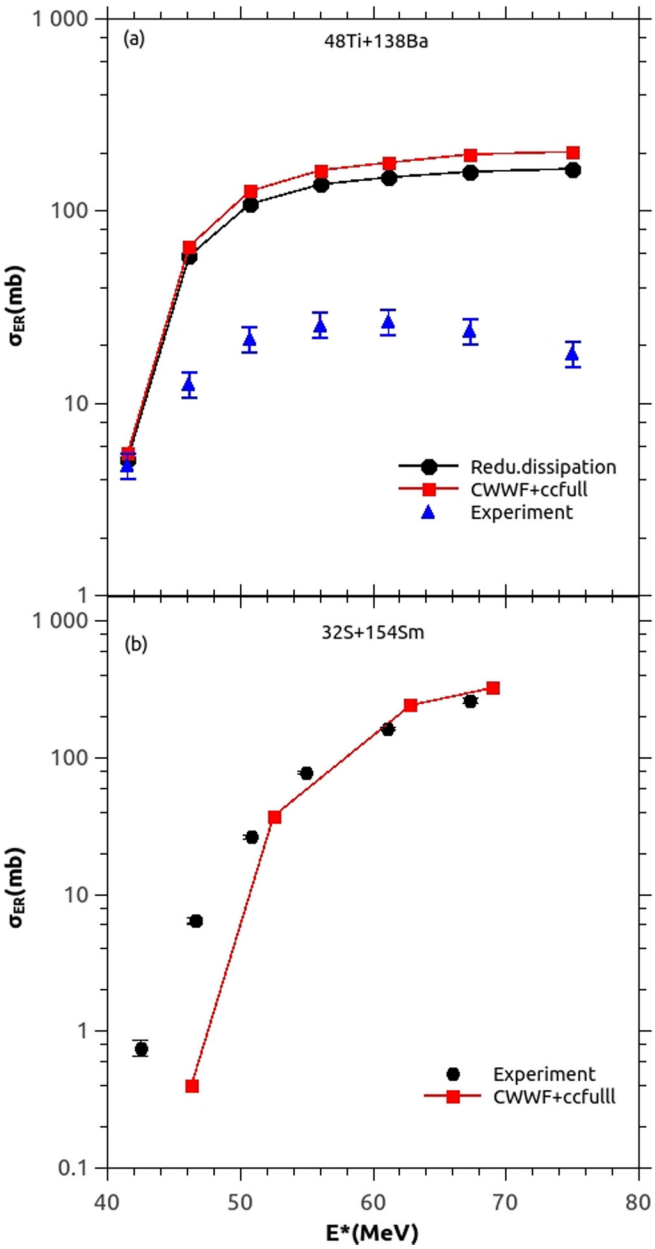

FIG. 4. Comparison of experimental ER cross sections for ^{48}Ti + ^{138}Ba (upper panel) and ^{32}S + ^{154}Sm (lower panel) with dynamical model calculations. The choices of inputs for the calculations are indicated.

system, forming the same compound nucleus, the calculation is performed for ^{32}S + ^{154}Sm also, where the measurement is already reported [54] and the result is shown in Fig. 4(b). (The parameters of the system are also given in Table II.) A comparatively better agreement is observed in case of the asymmetric channel. Next, for completeness, we have calculated the ER cross section for the symmetric channel with a constant reduced dissipation $\eta/m = 10^{21}$ s^{-1} and angular distribution from the systematics [Eq. (4)]. As depicted in Fig. 4, this set of calculation also confirms the suppression of experimental ER cross section for the symmetric system.

VI. DISCUSSION

The theoretical analysis of the reactions shows an over estimation of the ERs for the symmetric system. This discrepancy between the experimental results and the theoretical predictions can be explained as follows. The fusion cross sections, required for the present calculations, are estimated without incorporating any noncompound processes such as quasifission. Consequently, for the present target-projectile combination, the estimated fusion cross section is larger than the actual value. This may justify the presence of noncompound reaction mechanism in the ^{48}Ti + ^{138}Ba reaction.

Further, the measured ER cross sections are compared with the known results for ^{32}S + ^{154}Sm [54] reaction which forms the same CN, ^{186}Pt*. The nuclear reactions forming same CN through different entrance channels provide an opportunity for a systematic understanding of competing decay modes. The reduced ER cross sections of the reactions, as shown in Fig. 5(a), are considered for the comparison to eliminate any size effect that may appear in the absolute cross sections. To convert absolute cross sections(σ_{ER}) into reduced cross sections, σ_{ER} is divided by $\pi\lambda\!\!\!^{-2}$, where $\lambda\!\!\!^{-}$ is the reduced de Broglie wavelength of ER. The two reactions are compared

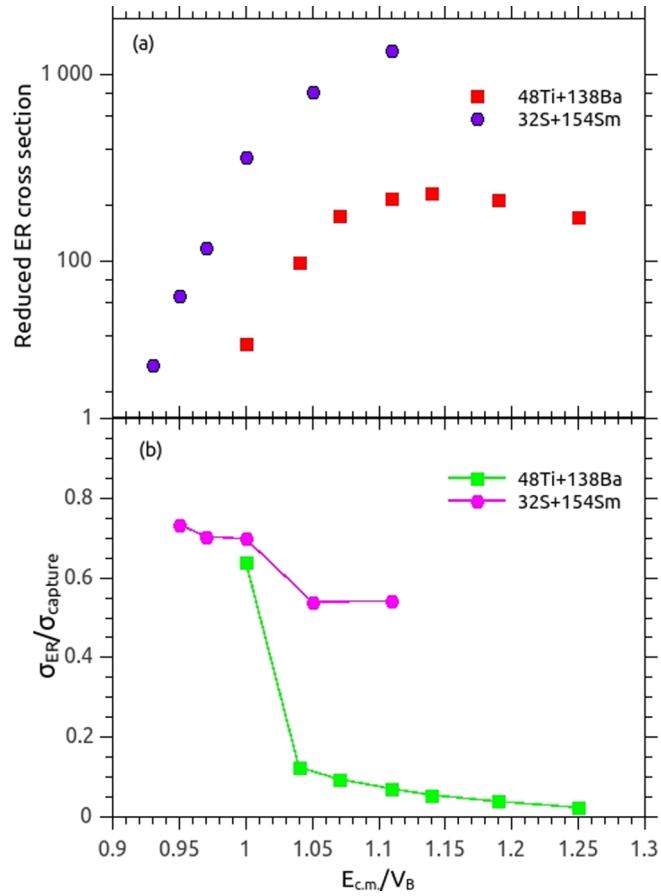

FIG. 5. (a) Upper panel: Comparison of reduced ER cross sections of ^{48}Ti + ^{138}Ba reaction with ^{32}S + ^{154}Sm. (b) Lower panel: Comparison of the ratio of ER cross section to the CCFULL predicted capture cross section for the same reactions. In both reactions, lines guide the eye.

for the same excitation energy range above the Coulomb barrier.

In Fig. 5(a), the ER cross section has a steady increasing trend with $\frac{E_{\mathrm{c.m.}}}{V_B}$ ratio for $^{32}\mathrm{S} + ^{154}\mathrm{Sm}$, while it is different for $^{48}\mathrm{Ti} + ^{138}\mathrm{Ba}$. This indicates a suppression in fusion probability, especially at higher energies for present system which is more symmetric compared to the other reaction. This result is consistent with the fact that mass asymmetry dependence of the potential energy surface can influence fusion probability [9,19,55]. In the case of mass asymmetric reactions, the driving force due to the nuclear potential favors absorption of the light projectile by the heavy target nucleus, which leads to a compact CN with high probability [14]. However, for mass symmetric reactions, system tends to become more symmetric through the mass flow from target to projectile and eventually the dinuclear system breaks without forming a shape equilibrated CN.

We next plot in Fig. 5(b), the experimental survival probability as the ratio of experimental ER cross section to the CCFULL predicted capture cross section for both reactions. The various input parameters used in the CCFULL calculations are shown Table IV. Capture cross section is the sum of fusion cross section and cross section for non-compound-nuclear reactions ($\sigma_{\mathrm{Cap}} = \sigma_{\mathrm{fus}} + \sigma_{\mathrm{NCN}}$). A high fission barrier prevent the system from decaying through fission (see Table II). So fusion cross section correspond to ER cross section (since $\sigma_{\mathrm{fus}} = \sigma_{\mathrm{fission}} + \sigma_{\mathrm{ER}}$), which has a decreasing trend. Thus the deviation of this ratio from unity suggest a lesser probability for fusion, enhancing the chances of the non-CN reaction. The survival probability of $^{32}\mathrm{S} + ^{154}\mathrm{Sm}$ has a moderate fall at higher excitation energies above Coulomb barrier, suggesting higher survival probability for the reaction. However, the survival probability of $^{48}\mathrm{Ti} + ^{138}\mathrm{Ba}$ system is substantially smaller and this suggest a lower probability for CN formation.

In the present study, both symmetric and asymmetric systems, forming the same compound nucleus, have same fission barrier (see Table II). A higher fission barrier reduces the probability of fission and increases the chances of decay of the compound nucleus through the evaporation of light particles. However, there is a decreasing trend in the ER cross sections in the present reaction at higher excitation energies. This points towards a fusion hindrance as ERs are the indisputable signature of fusion. According to dinuclear system (DNS) concept of nuclear fusion, this suppression in the fusion is interpreted as due to the presence of quasifission reaction [56–58]. In addition, for a more symmetric mass pair, the tendency of mass flow is towards the projectile creating a symmetric dinucleus before evolving into a mononucleus and fissioning through an asymmetric conditional saddle leading to quasifission [59].

The fusion hindrance can also be explained on the basis of mean fissility [5] (see Table II). The mean fissility represents the degree of reseparability of the dinuclear system, which is macroscopically determined by the Coulomb repulsion in the initial stage of the reaction and balance between surface and Coulomb energies of the compound system in the later stage of the reaction [8]. The calculations of mean fissility parameter depends on the entrance channel fissility and CN fissility. Even though CN fissility is same for both reactions, entrance channel fissilities will vary considerably as the angular momentum imparted by both projectiles are significantly different, even at the same excitation energies. The angular momentum imparted by the heavy projectile would be larger and this in turn decreases the fission barrier or increases the fissility. A higher mean fissility of symmetric system ($\chi_m = 0.66$) than that of the asymmetric system ($\chi_m = 0.54$) point towards a higher probability of reseparation of the symmetric system before the formation of a compound nucleus.

It has been shown that the fusion of massive reaction systems strongly depends on the shell structure of colliding partners [60]. The presence of shell closure or magic shells influence the reaction outcome as far as heavy systems are concerned. The compound nuclear formation probability increases when magic numbers are involved in the entrance channel [60,61]. This is due to the fact that magic nuclei are indeed expected to generate cold valleys in the potential energy surface, favoring the formation of a compact CN [62]. Further, magic nuclei are difficult to be excited, thereby reducing energy dissipation and then allowing the formation of a more compact dinuclear system [16]. In either explanation, it is clear that the heavy ion induced reactions involving shell structures in the input channel enhance the fusion probability. At the same time, there is instance of quasifission for reaction involving magic numbers in the entrance channel [22]. In the present study also, it is observed that the QF supersedes the shell closure effect of the target. Shell effects are also expected to be negligible at high excitation energies.

VII. SUMMARY

We have measured the ER cross sections for $^{48}\mathrm{Ti} + ^{138}\mathrm{Ba}$ at excitation energies in the range of 41–75 MeV and compared them with those of $^{32}\mathrm{S} + ^{154}\mathrm{Sm}$, both forming the same CN. The comparison has clearly shown the evidence of entrance channel effect with increasing values of charge product Z_pZ_t. While the theoretical analysis of the reactions shows a significant deviation of ER cross section from the experimental values for the symmetric system, it is in good agreement with asymmetric system. The depletion of ER cross sections for $^{48}\mathrm{Ti} + ^{138}\mathrm{Ba}$ at higher excitation energies as compared to that of $^{32}\mathrm{S} + ^{154}\mathrm{Sm}$ is a clear signature of the presence of non compound nuclear reaction such as fast fission, pre-equilibrium fission or quasifission. As fast fission is dominant at higher angular momenta with vanishingly small fission barrier heights and that the pre equilibrium fission takes place when the temperature of the system becomes comparable to the fission barrier, the reduction in the ER cross sections of the present study may be attributed to QF. In addition, it seems that the effect of target shell closure has no profound influence in the present reaction as there is no enhanced fusion probability at higher excitation energies.

ACKNOWLEDGMENTS

We thank the Pelletron and LINAC groups of IUAC for a commendable support during the entire run of the experiment and delivering an excellent quality of pulsed

beam. We acknowledge the support of the target laboratory of IUAC, especially S. R. Abhilash, in the fabrication of barium targets of fine quality and S. Ojha for the RBS study of the targets.

[1] Y. T. Oganessian and Y. A. Lazarev, in *Treatise on Heavy-Ion Science*, edited by D. A. Bromley (Plenum, New York, 1985), Vol. 4, p. 3.
[2] P. Armbruster, C. R. Phys. **4**, 571 (2003).
[3] W. J. Swiatecki, Phys. Scr. **24**, 113 (1981).
[4] S. Bjornholm and W. J. Swiatecki, Nucl. Phys. A **391**, 471 (1982).
[5] J. P. Blocki *et al.*, Nucl. Phys. A **459**, 145 (1986).
[6] D. J. Hinde, R. G. Thomas, R. du Rietz, A. Diaz-Torres, M. Dasgupta, M. L. Brown, M. Evers, L. R. Gasques, R. Rafiei, and M. D. Rodriguez, Phys. Rev. Lett. **100**, 202701 (2008).
[7] R. Rafiei, R. G. Thomas, D. J. Hinde, M. Dasgupta, C. R. Morton, L. R. Gasques, M. L. Brown, and M. D. Rodriguez, Phys. Rev. C **77**, 024606 (2008).
[8] R. G. Thomas, D. J. Hinde, D. Duniec, F. Zenke, M. Dasgupta, M. L. Brown, M. Evers, L. R. Gasques, M. D. Rodriguez, and A. Diaz-Torres, Phys. Rev. C **77**, 034610 (2008).
[9] A. C. Berriman, D. J. Hinde, M. Dasgupta, C. R. Morton, R. D. Butt, and J. O. Newton, Nature (London) **413**, 144 (2001).
[10] C. Yadav *et al.*, Phys. Rev. C **86**, 034606 (2012).
[11] V. S. Ramamurthy *et al.*, Phys. Rev. Lett. **65**, 25 (1990).
[12] J. C. Mein, D. J. Hinde, M. Dasgupta, J. R. Leigh, J. O. Newton, and H. Timmers, Phys. Rev. C **55**, R995(R) (1997).
[13] J. P. Lestone *et al.*, J. Phys. G **23**, 1349 (1997).
[14] D. J. Hinde, M. Dasgupta, and A. Mukherjee, Phys. Rev. Lett. **89**, 282701 (2002).
[15] R. P. Schmitt, L. Cooke, H. Dejbakhsh, D. R. Haenni, T. Shutt, B. K. Srivastava, and H. Utsunomiya, Nucl. Phys. A **592**, 130 (1995).
[16] D. J. Hinde and M. Dasgupta, Phys. Lett. B **622**, 23 (2005).
[17] K. Nishio, S. Mitsuoka, I. Nishinaka, H. Makii, Y. Wakabayashi, H. Ikezoe, K. Hirose, T. Ohtsuki, Y. Aritomo, and S. Hofmann, Phys. Rev. C **86**, 034608 (2012).
[18] D. J. Hinde, R. du Rietz, M. Dasgupta, R. G. Thomas, and L. R. Gasques, Phys. Rev. Lett. **101**, 092701 (2008).
[19] D. J. Hinde, M. Dasgupta, J. R. Leigh, J. C. Mein, C. R. Morton, J. O. Newton, and H. Timmers, Phys. Rev. C **53**, 1290 (1996).
[20] D. J. Hinde, M. Dasgupta, J. R. Leigh, J. P. Lestone, J. C. Mein, C. R. Morton, J. O. Newton, and H. Timmers, Phys. Rev. Lett. **74**, 1295 (1995).
[21] G. N. Knyazheva, E. M. Kozulin, R. N. Sagaidak, A. Y. Chizhov, M. G. Itkis, N. A. Kondratiev, V. M. Voskressensky, A. M. Stefanini, B. R. Behera, L. Corradi, E. Fioretto, A. Gadea, A. Latina, S. Szilner, M. Trotta, S. Beghini, G. Montagnoli, F. Scarlassara, F. Haas, N. Rowley, P. R. S. Gomes, and A. Szantode Toledo, Phys. Rev. C **75**, 064602 (2007).
[22] C. Simenel, D. J. Hinde, R. du Rietz, M. Dasgupta, M. Evers, C. J. Lin, D. H. Luong, and A. Wakhle, Phys. Lett. B **710**, 607 (2012).
[23] A. Wakhle, C. Simenel, D. J. Hinde, M. Dasgupta, M. Evers, D. H. Luong, R. du Rietz, and E. Williams, Phys. Rev. Lett. **113**, 182502 (2014).
[24] R. G. Thomas, R. K. Choudhury, A. K. Mohanty, A. Saxena, and S. S. Kapoor, Phys. Rev. C **67**, 041601(R) (2003).
[25] R. K. Choudhury and R. G. Thomas, J. Phys.: Conf. Ser. **282**, 012004 (2011).
[26] P. D. Shidling, N. Madhavan, V. S. Ramamurthy, S. Nath, N. M. Badiger, S. Pal, A. K. Sinha, A. Jhingan, S. Muralithar, P. Sugathan, S. Kailas, B. R. Behera, R. Singh, K. M. Varier, and M. C. Radhakrishna, Phys. Lett. B **670**, 99 (2008).
[27] V. S. Ramamurthy and S. S. Kapoor, Phys. Rev. Lett. **54**, 178 (1985).
[28] S. Soheyli and M. K. Khalili, Phys. Rev. C **85**, 034610 (2012).
[29] Y. Ts. Oganessian *et al.* Phys. Rev. Lett. **104**, 142502 (2010).
[30] T. K. Ghosh, A. Chaudhuri, K. Banerjee, S. Bhattacharya, C. Bhattacharya, S. Kundu, G. Mukherjee, R. Pandey, T. K. Rana, P. Roy, T. Roy, V. Srivastava, and P. Bhattacharya, Pramana **85**, 291 (2015).
[31] K. K. Rajesh, M. M. Musthafa, M. M. Hosamani, A. Shamlath, S. R. Abhilash, and D. Kabiraj, Vacuum **141**, 230 (2017).
[32] N. Madhavan, S. Nath, T. Varughese, J. Gehlot, A. Jhingan, P. Sugathan, A. K. Sinha, R. Singh, K. M. Varier, M. C. Radhakrishna, E. Prasad, S. Kalkal, G. Mohanto, J. J. Das, R. Kumar, R. P. Singh, S. Muralithar, R. K. Bhowmik, A. Roy, Rajesh Kumar, S. K. Suman, A. Mandal, T. S. Datta, J. Chacko, A. Choudhury, U. G. Naik, A. J. Malyadri, M. Archunan, J. Zacharias, S. Rao, M. Kumar, P. Barua, E. T. Subramanian, K. Rani, B. P. Ajith Kumar, and K. S. Golda, Pramana **75**, 317 (2010).
[33] E. Prasad, K. M. Varier, N. Madhavan, S. Nath, J. Gehlot, S. Kalkal, J. Sadhukhan, G. Mohanto, P. Sugathan, A. Jhingan, B. R. S. Babu, T. Varughese, K. S. Golda, B. P. Ajith Kumar, B. Satheesh, S. Pal, R. Singh, A. K. Sinha, and S. Kailas, Phys. Rev. C **84**, 064606 (2011).
[34] S. Nath, Comput. Phys. Commun. **179**, 492 (2008); **180**, 2392 (2009).
[35] A. Jhinghan, Pramana **85**, 483 (2015).
[36] E. T. Subramanium, B. P. Ajith Kumar, and R. K. Bhowmik, CANDLE: Collection and Analysis of Nuclear Data using Linux Network, http://www.iuac.res.in/NIAS.
[37] G. Mohanto, N. Madhavan, S. Nath, J. Gehlot, I. Mukul, A. Jhingan, T. Varughese, A. Roy, R. K. Bhowmik, I. Mazumdar, D. A. Gothe, P. B. Chavan, J. Sadhukhan, S. Pal, Maninder Kaur, Varinderjit Singh, A. K. Sinha, and V. S. Ramamurthy, Phys. Rev. C **88**, 034606 (2013).
[38] V. Singh, B. R. Behera, M. Kaur, A. Kumar, K. P. Singh, N. Madhavan, S. Nath, J. Gehlot, G. Mohanto, A. Jhingan, I. Mukul, T. Varughese, J. Sadhukhan, S. Pal, S. Goyal, A. Saxena, S. Santra, and S. Kailas, Phys. Rev. C **89**, 024609 (2014).
[39] R. Sandal, B. R. Behera, V. Singh, M. Kaur, A. Kumar, G. Kaur, P. Sharma, N. Madhavan, S. Nath, J. Gehlot, A. Jhingan, K. S. Golda, H. Singh, S. Mandal, S. Verma, E. Prasad, K. M. Varier, A. M. Vinodkumar, A. Saxena, J. Sadhukhan, and S. Pal, Phys. Rev. C **91**, 044621 (2015).
[40] P. Sharma, B. R. Behera, R. Mahajan, M. Thakur, G. Kaur, K. Kapoor, K. Rani, N. Madhavan, S. Nath, J. Gehlot, R. Dubey, I. Mazumdar, S. M. Patel, M. Dhibar, M. M. Hosamani, Khushboo, N. Kumar, A. Shamlath, G. Mohanto, and S. Pal, Phys. Rev. C **96**, 034613 (2017).
[41] http://lise.nscl.msu.edu/pace4.
[42] J. Sadhukhan and S. Pal, Phys. Rev. C **81**, 031602(R) (2010).
[43] P. Fröbrich and I. I. Gontchar, Phys. Rep. **292**, 131 (1998).

[44] Y. Abe, S. Ayik, P.-G. Reinhard, and E. Suraud, Phys. Rep. **275**, 49 (1996).
[45] K. T. R. Davies, R. A. Managan, J. R. Nix, and A. J. Sierk, Phys. Rev. C **16**, 1890 (1977).
[46] J. Sadhukhan and S. Pal, Phys. Rev. C **84**, 044610 (2011).
[47] W. Reisdorf, Z. Phys. A **300**, 227 (1981).
[48] A. J. Sierk, Phys. Rev. C **33**, 2039 (1986).
[49] K. Hagino, N. Rowley, and A. T. Kruppa, Comput. Phys. Commun. **123**, 143 (1999).
[50] M. Brack, J. Damgaard, A. S. Jensen, H. C. Pauli, V. M. Strutinsky, and C. Y. Wong, Rev. Mod. Phys. **44**, 320 (1972).
[51] V. Weisskopf, Phys. Rev. **52**, 295 (1937).
[52] J. D. Lynn, *The Theory of Neutron Resonance Reactions* (Clarendon Press, Oxford, 1968).
[53] S. Pal and T. Mukhopadhyay, Phys. Rev. C **57**, 210 (1998).
[54] P. R. S. Gomes, I. C. Charret, R. Wanis, G. M. Sigaud, V. R. Vanin, R. Liguori Neto, D. Abriola, O. A. Capurro, D. E. DiGregorio, M. di Tada, G. Duchene, M. Elgue, A. Etchegoyen, J. O. Fernandez Niello, A. M. J. Ferrero, S. Gil, A. O. Macchiavelli, A. J. Pacheco, and J. E. Testoni, Phys. Rev. C **49**, 245 (1994).
[55] R. A. Broglia and A. Winther, *Heavy Ion Reaction Lecture Notes, Vol. 1: Elastic and Inelastic Reactions* (Benjamin/ Cummings, Reading, MA, 1981).
[56] G. G. Adamian, in *Nuclear Theory 22-Conference Paper*, edited by V. Nikolaev (Heron Press, Sofia, 2003), p. 259.
[57] A. Nasirov, G. Giardina, G. Mandaglio, M. Manganaro, and W. Scheid, J. Phys.: Conf. Series **282**, 012010 (2011).
[58] T. K. Ghosh, A. Chaudhuri, K. Banerjee, S. Bhattacharya, C. Bhattacharya, S. Kundu, G. Mukherjee, R. Pandey, T. K. Rana, P. Roy, T. Roy, V. Srivastava, and P. Bhattacharya, Pramana - J. Phys. **85**, 2 (2015).
[59] H. W. Gäggeler, T. Sikkeland, G. Wirth, W. Brüchle, W. Bögl, G. Franz, G. Herrmann, J. V. Kratz, M. Schädel, K. Sümmerer, and W. Weber, Z. Phys. A: At. Nucl. **316**, 291 (1984).
[60] K. Satou, H. Ikezoe, S. Mitsuoka, K. Nishio, and S. C. Jeong, Phys. Rev. C **65**, 054602 (2002).
[61] G. Mohanto, D. J. Hinde, K. Banerjee, M. Dasgupta, D. Y. Jeung, C. Simenel, E. C. Simpson, A. Wakhle, E. Williams, I. P. Carter, K. J. Cook, D. H. Luong, C. S. Palshetkar, and D. C. Rafferty, Phys. Rev. C **97**, 054603 (2018).
[62] A. Sandulescu, R. Gupta, W. Scheid, and W. Greiner, Phys. Lett. B **60**, 225 (1976).